AIP | Applied Physics Letters

Stress compensation for arbitrary curvature control in vanadium dioxide phase transition actuators

Kaichen Dong, Shuai Lou, Hwan Sung Choe, Kai Liu, Zheng You, Jie Yao, and Junqiao Wu

Citation: Applied Physics Letters **109**, 023504 (2016); doi: 10.1063/1.4958692
View online: http://dx.doi.org/10.1063/1.4958692
View Table of Contents: http://scitation.aip.org/content/aip/journal/apl/109/2?ver=pdfcov
Published by the AIP Publishing

APPLIED PHYSICS LETTERS **109**, 023504 (2016)

Stress compensation for arbitrary curvature control in vanadium dioxide phase transition actuators

Kaichen Dong,[1,2,3,a)] Shuai Lou,[1,2] Hwan Sung Choe,[1,2] Kai Liu,[4] Zheng You,[3] Jie Yao,[1,2] and Junqiao Wu[1,2,a)]

[1]*Department of Materials Science and Engineering, University of California, Berkeley, California 94720, USA*
[2]*Materials Sciences Division, Lawrence Berkeley National Laboratory, Berkeley, California 94720, USA*
[3]*State Key Laboratory of Precision Measurement Technology and Instruments, Department of Precision Instrument, Tsinghua University, Beijing 100084, People's Republic of China*
[4]*School of Materials Science and Engineering, Tsinghua University, Beijing 100084, People's Republic of China*

(Received 4 May 2016; accepted 30 June 2016; published online 12 July 2016)

Due to its thermally driven structural phase transition, vanadium dioxide (VO_2) has emerged as a promising material for micro/nano-actuators with superior volumetric work density, actuation amplitude, and repetition frequency. However, the high initial curvature of VO_2 actuators severely obstructs the actuation performance and application. Here, we introduce a "seesaw" method of fabricating tri-layer cantilevers to compensate for the residual stress and realize nearly arbitrary curvature control of VO_2 actuators. By simply adjusting the thicknesses of the individual layers, cantilevers with positive, zero, or negative curvatures can be engineered. The actuation amplitude can be decoupled from the curvature and controlled independently as well. Based on the experimentally measured residual stresses, we demonstrate sub-micron thick VO_2 actuators with nearly zero final curvature and a high actuation amplitude simultaneously. This "seesaw" method can be further extended to the curvature engineering of other microelectromechanical system multi-layer structures where large stress-mismatch between layers are inevitable. *Published by AIP Publishing.*
[http://dx.doi.org/10.1063/1.4958692]

Micro- and nano-actuators are widely used in reconfigurable metamaterials,[1] microelectromechanical systems (MEMSs), and nanoelectromechanical systems (NEMSs), such as electrical switches[2] and micro-mirror arrays.[3] To optimize the performance of those devices, large amplitude and strong, high speed force output are required. Vanadium dioxide (VO_2) has emerged as a promising actuator working material with superior overall performance.[4–9] This is because VO_2 undergoes a metal-insulator phase transition (MIT) at a temperature slightly above room temperature (67 °C) that causes a significant shrinkage of the crystal along the *C*-axis of its rutile phase, thus leading to a large strain transformation and high work density.[4–14]

In spite of these attractive properties of VO_2 actuators, these devices suffer from large residual stress mismatch between VO_2 and the clamping materials in a multi-layer structure.[5,8,15] Previous work on VO_2 actuators generally utilize two fabrication approaches, pre-release deposition[5,8] and post-release deposition[4,6,7,9,12,13,15,16] of VO_2 films. In the pre-release deposition approach, VO_2 is first deposited on thermal oxide. Then, a metal layer (e.g., Cr) is deposited onto the VO_2 layer, followed by etching to define the anchor and actuator pattern. This approach uses conventional fabrication techniques, but the high built-in residual stress in Cr leads to a high initial curvature.[5,8] In the post-release deposition approach, VO_2 films are grown directly on released cantilever structures[7,15] or atomic-force microscopy (AFM) probes.[4,13,16] This method also results in a high initial curvature due to the built-in stress within the VO_2 layers. Since these approaches in previous work are based on stress-mismatched bi-layer configurations, neither of them realizes arbitrary control of VO_2 actuator curvatures or the elimination of the high initial curvature. However, nearly zero and controllable curvatures are critically important in many position/curvature-sensitive micro/nano-devices.[17–19] For example, some reconfigurable nanomechanical metamaterials utilize geometrically tunable metallic gaps to adjust the transmission coefficient. With a near zero-curvature suspended structure, the performance will be enhanced with a small and controllable gap.[17] Surface machined MEMS switches also require the cantilever to default to near zero curvature to make the top and bottom electrodes easier to contact each other.[2,20] A high initial curvature in VO_2 cantilevers severely impedes the wide application of VO_2-based actuators.

For conventional multi-layer structures in MEMSs, many stress engineering techniques are used to solve the high initial curvature problem. However, such techniques usually involve additional, complex fabrication processes, such as deposition parameter optimization,[21–23] thermal annealing,[24] ion implantation,[25] or different deposition methods.[26] Since VO_2 is sensitive to high temperature and oxidation environments, these stress engineering processes not only elevate the fabrication complexity and cost of VO_2 devices, but also may degrade the physical properties of VO_2 films. Moreover, deposition of high-quality VO_2 requires high temperature,[4–16] which limits the selection of underlayer materials, making it more difficult to find a stress-matched material with VO_2 and further limits the VO_2 actuator fabrication.

[a)]Authors to whom correspondence should be addressed. Electronic addresses: dkc12@mails.tsinghua.edu.cn and wuj@berkeley.edu

In this work, we demonstrate a way to control the curvature of VO_2-based actuators using a "seesaw" method with a tri-layer cantilever structure. Thin layers with different residual stresses are used to build the tri-layer actuator. Our rational design of the thickness ratios among the three layers realizes a nearly arbitrary control of the curvature. This work is based on the pre-release deposition approach, and no additional stress engineering processes or microfabrication techniques are needed. Furthermore, this method achieves independent control of the initial curvature and the insulating (I) to metallic (M) phase curvature change, which greatly facilitates the design of VO_2-based devices. First, we analyze the limits of the conventional bi-layer VO_2 actuators. In comparison with the bi-layer design, the "seesaw" tri-layer design is introduced to overcome the curvature control limits within conventional bi-layer structures. We then analyze the curvature control of tri-layer actuators and compare their performance to the bi-layer counterpart. We experimentally measure the residual stresses of all materials involved in our devices. Finally, based on the fabrication design and residual stress information, Au/Cr/VO_2 tri-layer actuators are fabricated and tested, and the experimental results are found to agree with our simulation design.

Figure 1(a) shows a schematic diagram of bi-layer cantilever VO_2 actuators, which are formed by mechanically coupling a VO_2 layer with another material without phase transition. The curvature of the actuator greatly changes when the VO_2 layer switches from its I-phase to M-phase. However, due to the residual stress mismatch between the two layers, the VO_2 actuators typically exhibit an unwanted initial curvature when it is released. To simulate the curvature of the bi-layers, we utilize the model by Nikishkov[27] to calculate the curvature of Cr/VO_2 and Au/VO_2 bi-layer cantilevers

$$K=\frac{3\sum_{n=1}^{m}E'_n t_n(y_n+y_{n-1}-2y_b)(c-(1+\nu_n)\varepsilon_n)}{2\sum_{n=1}^{m}E'_n t_n\left[{y_n}^2+y_n y_{n-1}+{y_{n-1}}^2-3y_b(y_n+y_{n-1}-y_b)\right]}, \tag{1}$$

$$y_b=\left[\sum_{n=1}^{m}E'_n t_n(y_n+y_{n-1})\right]\Big/\left(2\sum_{n=1}^{m}E'_n t_n\right), \tag{2}$$

$$c=\left[\sum_{n=1}^{m}E'_n t_n(1+\nu_n)\varepsilon_n\right]\Big/\left(\sum_{n=1}^{m}E'_n t_n\right), \tag{3}$$

where K is the cantilever curvature, m is the total number of layers in the cantilever, $E'_n=E_n/(1-{\nu_n}^2)$, $y_n=y_{n-1}+t_n$, and $y_0=0$. The material properties involved are Young's modulus E_n, Poisson's ratio ν_n, film thickness t_n, and initial strain ε_n of the nth layer. Note that the initial strain can be calculated by the residual stress and material elastic properties.

The analytical results for both the I-phase and M-phase of VO_2 are shown in Figure 1(b). Note that thermal expansion is neglected here because it only induces a small curvature change compared to that caused by residual stresses and the VO_2 phase transition.[5] For the calculated results shown in Figure 1, material properties (elastic modulus and Poisson's ratio) were obtained from previous reports,[15,28,29] and other parameters (film thickness, residual stress, etc.) were taken from our experiments, unless otherwise specified. To accurately design the VO_2 strain change during the phase transition, we first utilized a lumped method by fitting an "effective stress change" during the VO_2 phase transition with experimental data and used it in the following analytical discussion and device design.[15] Cr and Au are selected as the

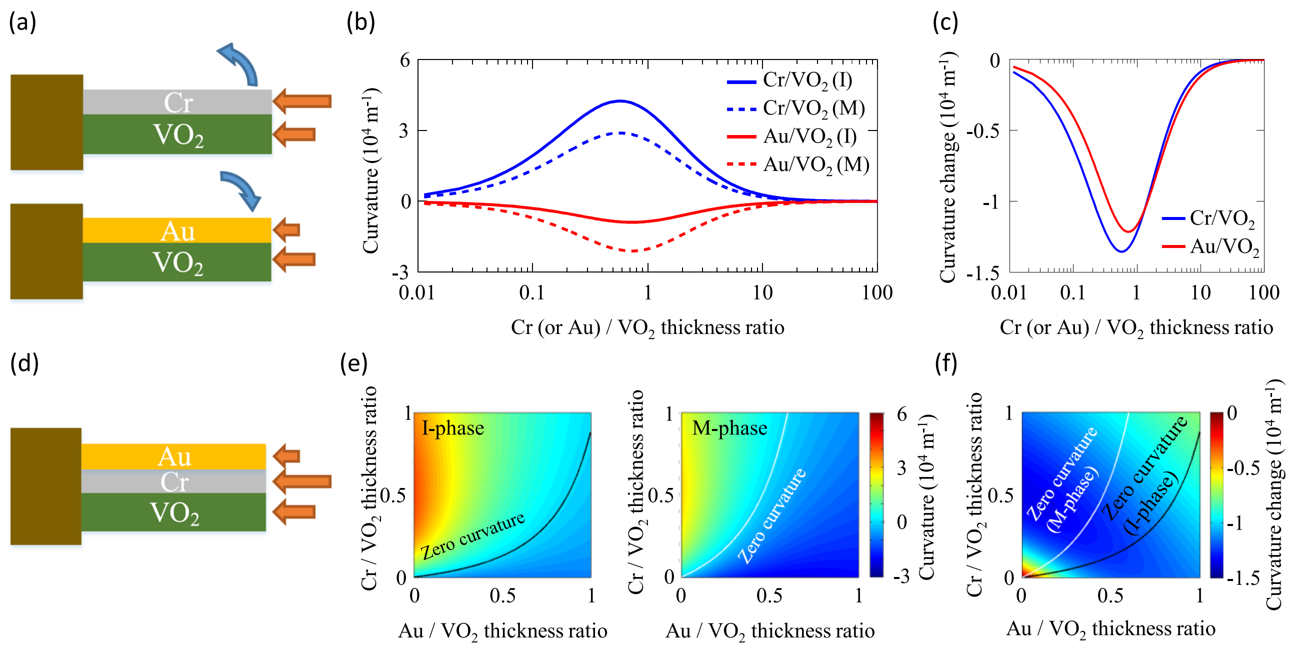

FIG. 1. Analytical comparison between bi-layer and tri-layer VO_2 actuators. (a) Schematic diagram of a Cr/VO_2 and an Au/VO_2 bi-layer actuator, where residual stresses cause unwanted initial curvatures. The orange arrows indicate the strain change of each layer after release (same in (d)), while the blue arrows indicate the cantilever bending direction (i.e., sign of curvature). (b) Calculated curvature of Cr/VO_2 and Au/VO_2 bi-layer actuators when the VO_2 is in the I-phase or M-phase. (c) Curvature change between the I-phase and M-phase of VO_2 for Cr/VO_2 and Au/VO_2 bi-layer actuators. (d) Schematic diagram of an Au/Cr/VO_2 tri-layer actuator. (e) Calculated curvature of Au/Cr/VO_2 tri-layer actuators when the VO_2 is in the I-phase or M-phase. The lines represent the contour where the curvature equals zero (same in (f)). (f) Curvature change between the I-phase and M-phase of Au/Cr/VO_2 tri-layer actuators.

clamping materials because they are widely used in a variety of reconfigurable metamaterials and MEMS/NEMS related applications.[1,28] Moreover, the residual stresses in Cr and Au are larger and smaller than that in VO_2, respectively. Figure 1(b) clearly shows that the VO_2 bi-layer system tends to bend towards the side with larger initial built-in tensile stress and hence exhibits a large curvature. Here, we define the positive curvature as an upward bend in the cantilever. Regardless of the thickness ratios of the layers, the curvature never changes its sign or even reaches zero. The peak value appears at the thickness ratio of $\sim$0.6 for Cr/VO_2 and $\sim$0.7 for Au/VO_2.[5,10] Since a large curvature change defines a greater stroke and a better performance of the actuator, we further compute the curvature change of the bi-layer VO_2 actuators between the I-phase and M-phase, as shown in Figure 1(c). The curvature change is calculated as the M-phase curvature minus the I-phase curvature and has a linear relationship with the I-phase or M-phase curvatures themselves. If the thickness of either layer dominates (with a thickness ratio far from 1), the total curvature and the curvature change decrease simultaneously. Therefore, in this bi-layer configuration, it is not possible to achieve a flat curvature (in either I-phase or M-phase) without sacrificing the net curvature change.

To solve this problem, here we introduce the tri-layer configuration. As depicted in Figure 1(d), the Cr layer, which possesses the largest residual stress, is sandwiched by an Au and a VO_2 layer, which have smaller stresses, forming a "seesaw" structure in terms of stress compensation. Within a certain range, arbitrary curvatures can be achieved by simply adjusting the thickness ratios between the three layers.[26] Based on the Equations (1)–(3), we plot, in Figure 1(e), the calculated curvature of Au/Cr/VO_2 actuators when the VO_2 is in the I- or M-phase, which proves that adjusting the thickness of either or both layers (Cr and Au) results in curvatures with different signs or zero value. Note that the bi-layer cases correspond to the horizontal and vertical axes in Figure 1(e), which means that the limit of curvature adjustment in the tri-layer case is the bi-layer configuration. In Figure 1(f), we show the curvature change of tri-layer VO_2 actuators between the M-phase and I-phase. It is shown that there is no degradation in the actuation performance, when compared to the bi-layer configuration, if it is carefully designed. The maximum curvature change of a tri-layer VO_2 actuator with zero curvature in the M-phase is roughly $-1.31 \times 10^4\,\mathrm{m}^{-1}$, while the peak values of Cr/VO_2 and Au/VO_2 structures are $-1.35 \times 10^4\,\mathrm{m}^{-1}$ and $-1.21 \times 10^4\,\mathrm{m}^{-1}$, respectively. By designing the thickness ratio in the tri-layer actuator, we can achieve zero curvature in either M-phase or I-phase, whereas the curvature change is nearly arbitrarily adjustable as well. The independent control of the initial curvature and the I-M phase curvature change greatly expands the MEMS/NEMS design space and widens the applications of VO_2 actuators.

To determine the residual stresses in individual layers for the tri-layer design, we used the free-standing cantilever method.[30,31] We separately deposited Au, Cr, or VO_2 layers onto silicon cantilevers (NANOSENSOR Co., NCHR-W) and used an optical profilometer (ADE Phase Shift MicroXAM Optical interferometric profiler) to measure the cantilever

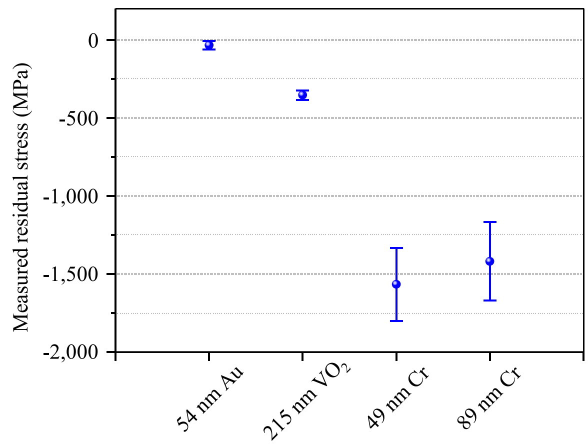

FIG. 2. Measured residual stresses of the Au, VO_2, and Cr films with different thicknesses involved in this work. Note that the negative value indicates a tensile residual stress developed within the film.

curvature after the thin film deposition. Based on these results, numerical calculations in COMSOL™ Multiphysics were used to retrieve the residual stresses within the deposited films, and the results are presented in Figure 2. The calculated residual stresses in Cr, Au, and VO_2 thin films agree well with previous reports.[28,32–34]

We also experimentally tested the curvature control and performance of the tri-layer VO_2 actuators. The fabrication process, as shown in Figure 3(a), started with a deposition of 170 nm VO_2 on a Si substrate with a 1 μm thick thermal oxide (SiO_2) by pulsed laser deposition (PLD). A krypton fluoride excimer laser ($\lambda = 248$ nm) was focused on a VO_2 target (99%) with a fluence of 350 mJ and a repetition rate of 5 Hz. The substrate temperature was kept at 575 °C, and the total oxygen pressure was 7 mTorr during the deposition. The 44 nm Au and 33 nm Cr deposition and patterning were done by photolithography, e-beam evaporation, and lift-off. Then, the anchor area was defined by photolithography using S1818 photoresist. The S1818 photoresist and Au/Cr layers served as masks in the following reactive ion etching (RIE), which etched the exposed VO_2 film with minimal lateral etching. Afterwards, the whole substrate was treated with buffered oxide etchant (BOE, 5:1) for a period of time, which etched part of the SiO_2 beneath the cantilevers without fully releasing the cantilevers. Since the initial curvature of our design is quite small compared to that of previous

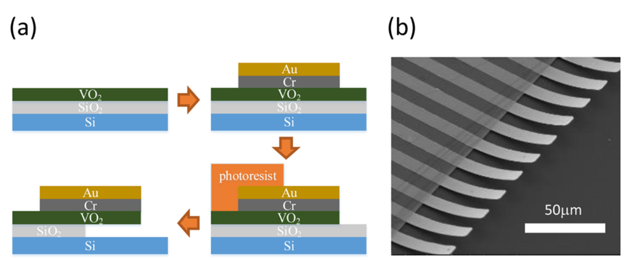

FIG. 3. Fabrication of VO_2 tri-layer cantilever actuators. (a) Deposit VO_2 film on the Si substrate with a 1 μm thick thermal oxide overlayer. E-beam evaporation of Cr and Au layers and lift-off. Define the anchor region using the photoresist and the RIE patterning of VO_2. Wet etch the sacrificial layer with BOE (5:1), remove photoresist with acetone, and then dry etch the residual thermal oxide with HF vapor. The thicknesses of the layers are not scaled. (b) SEM image of a released VO_2 actuator array.

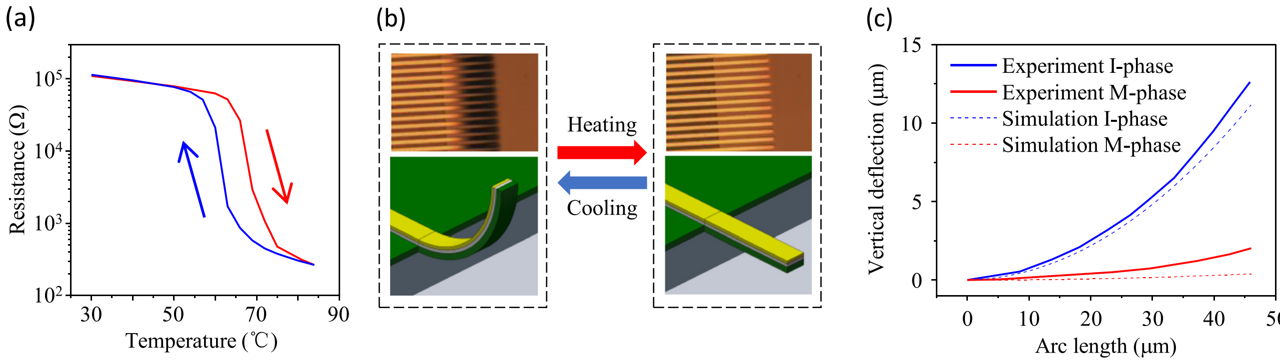

FIG. 4. Experimental results of the Au/Cr/VO_2 tri-layer actuator. (a) Temperature-dependent resistivity of a representative VO_2 film used, showing clear metal-insulator phase transition around 67 °C. The following characterizations were done at room temperature (~25 °C) or 85 °C, where VO_2 is fully in its I-phase or M-phase, respectively. (b) Optical images of VO_2 tri-layer actuators with corresponding schematic diagrams. (c) Comparison of experimental and simulated cantilever deflection, in both the I-phase and M-phase of VO_2. Note that, for a clear comparison, only part of the beam profiles are plotted.

work,[5,8] severe stiction between the cantilevers and the bottom substrate was observed if we completely released the cantilevers using the wet etching method and directly took them out. Instead, we applied HF vapor to fully release the suspended structures, following the removal of the photoresist by acetone. The VO_2 that covers the anchor area well protected the underlying SiO_2 and thus defined the anchor during the HF vapor etching process. We carefully controlled the HF vapor etching time because it may create a negative influence on VO_2 actuators. Critical point drying can also be used to release such structures. An SEM image of the released cantilevers is shown in Figure 3(b).

Depicted in Figure 4(a) is the resistance of a representative VO_2 film used as a function of temperature, confirming the expected I-M phase transition. The shape of the VO_2 tri-layer actuator was measured at room temperature (~25 °C) and 85 °C, where the VO_2 film was completely in its I-phase and M-phase, respectively. To help the release of the suspended structure, we intentionally designed the VO_2 tri-layer actuator to bend upwards at low temperature (I-phase). When the actuator was globally heated up beyond the phase transition temperature (reaching the M-phase), the in-plane shrinkage of the VO_2 layer actuated the entire cantilever and bent it downwards, reaching a nearly zero curvature. The cantilever profile was observed with a reflective microscope, as shown in Figure 4(b). To quantify the curvatures driven by the phase transition, we measured the cantilever profile with an optical microscope. Shown in Figure 4(c) is the comparison between the experimental results and numerical simulation by COMSOL. The VO_2 actuator achieved a curvature of $1.9 \times 10^3\ m^{-1}$ in its M-phase with a curvature change of $-9.3 \times 10^3\ m^{-1}$ across the phase transition. The slight discrepancies between the measured and the simulated curvatures are attributed to a few factors: (1) inaccuracy in the actual thicknesses of Au, Cr, and VO_2 layers, (2) error in the estimated residual stress of each layer, and (3) uncertainty in the phase transition stress in the VO_2 layer. Using slightly different thicknesses of Au and Cr by -3 nm and $+4$ nm, respectively, the experimental result can be perfectly fitted with the simulation result, which also shows the sensitivity of the curvature to thickness variations.

In summary, a "seesaw" method to compensate residual stress is proposed and implemented in an Au/Cr/VO_2 tri-layer cantilever structure to realize full control of the curvature of VO_2 phase-transition actuators. The curvature can be designed to be arbitrarily positive, zero, or negative by simply tuning the thickness ratio among the three layers involved. Moreover, the actuation amplitude of the VO_2 actuator, determined by the curvature change between the I-phase and M-phase state of the VO_2 layer, can be decoupled from the initial curvature value itself. The nearly arbitrary and decoupled control of VO_2 actuator curvatures and actuation amplitudes show the potential to greatly expand the applications of VO_2 actuators in such fields as reconfigurable metamaterials, MEMSs, and NEMSs.

This work was supported by the U.S. Department of Energy Early Career Award No. DE-FG02–11ER46796. Some of the measurements and device fabrication used facilities in the Lawrence Berkeley National Laboratory, which was supported by the Office of Science, Office of Basic Energy Sciences of the U.S. Department of Energy under Contract No. DE-AC02–05CH11231. Partial measurement and fabrication were done in the U.C. Berkeley Marvell Nanolab and Biomolecular Nanotechnology Center. J.W., J.Y. and K.D. acknowledge support from the Tsinghua-Berkeley Funds. K.D. acknowledges the China Scholarship Council (CSC, No. 201406210211) for financial support. The authors would thank K. Wang, C. Ko, X. Wang, Y. Chen, Z. Hou, P. Dong, X. Lei, K. Tom, and Y. Liu for helpful discussions.

[1]N. I. Zheludev and E. Plum, Nat. Nanotechnol. **11**, 16 (2016).
[2]P. Li, Z. You, and T. Cui, Appl. Phys. Lett. **101**, 093111 (2012).
[3]A. Tuantranont, L. Liew, V. M. Bright, W. Zhang, and Y. C. Lee, Sens. Actuators, A **89**, 124 (2001).
[4]A. Rúa, F. E. Fernández, and N. Sepúlveda, J. Appl. Phys. **107**, 074506 (2010).
[5]K. Liu, C. Cheng, Z. Cheng, K. Wang, R. Ramesh, and J. Wu, Nano Lett. **12**, 6302 (2012).
[6]R. Cabrera, E. Merced, and N. Sepúlveda, Phys. Status Solidi A **210**, 1704 (2013).
[7]E. Merced, X. Tan, and N. Sepúlveda, J. Microelectromech. Syst. **24**, 1073 (2014).
[8]K. Liu, C. Cheng, J. Suh, R. Tang-Kong, D. Fu, S. Lee, J. Zhou, L. O. Chua, and J. Wu, Adv. Mater. **26**, 1746 (2014).
[9]E. Merced, D. Torres, X. Tan, and N. Sepúlveda, J. Microelectromech. Syst. **24**, 100 (2015).
[10]J. Cao, W. Fan, Q. Zhou, E. Sheu, A. Liu, C. Barrett, and J. Wu, J. Appl. Phys. **108**, 083538 (2010).
[11]B. Viswanath and S. Ramanathan, Nanoscale **5**, 7484 (2013).

[12]E. Merced, J. Zhang, X. Tan, and N. Sepúlveda, IEEE/ASME Trans. Mechatronics **19**, 1583 (2013).
[13]J. Zhang, E. Merced, N. Sepúlveda, and X. Tan, IEEE/ASME Trans. Mechatronics **19**, 579 (2014).
[14]T. Wang, D. Torres, F. E. Fernández, A. Green, C. Wang, and N. Sepúlveda, ACS Nano **9**, 4371 (2015).
[15]R. Cabrera, E. Merced, and N. Sepúlveda, J. Microelectromech. Syst. **23**, 243 (2014).
[16]C. Ramsey, R. Cabrera, E. Merced, and N. Sepúlveda, in *IEEE Nanotechnology Materials and Devices Conference (NMDC)*, Hawaii, USA, 16–19 October (2012), pp. 120–123.
[17]J. Ou, E. Plum, J. Zhang, and N. I. Zheludev, Nat. Nanotechnol. **8**, 252 (2013).
[18]P. Cencillo, J. Y. Ou, J. Valente, E. Plum, and N. I. Zheludev, in 5th International Topical Meeting on Nanophotonics and Metamaterials 2015, Seefeld, Austria, 5–8 January (2015).
[19]J. Y. Ou, E. Plum, L. Jiang, and N. I. Zheludev, Nano Lett. **5**, 2142 (2011).
[20]G. M. Rebeiz and J. B. Muldavin, IEEE Microwave Mag. **2**, 59 (2001).
[21]S. M. Hu, J. Appl. Phys. **70**, R53 (1991).
[22]B. Bhushan, S. P. Murarka, and J. Gerlach, J. Vac. Sci. Technol., B **8**, 1068 (1990).
[23]E. A. Irene, J. Electron. Mater. **5**, 287 (1976).
[24]S. Huang, B. Li, and X. Zhang, Sens. Actuators, A **130–131**, 331 (2006).
[25]T. G. Bifano, H. T. Johnso, P. Bierden, and R. K. Mali, J. Microelectromech. Syst. **11**, 592 (2002).
[26]R. Liu, B. Jiao, Y. Kong, Z. Li, H. Shang, D. Lu, C. Gao, and D. Chen, J. Micromech. Microeng. **23**, 095019 (2013).
[27]G. P. Nikishkov, J. Appl. Phys. **94**, 5333 (2003).
[28]P. Tyagi, N. Bassik, T. G. Leong, J. H. Cho, B. R. Benson, and D. H. Gracias, J. Microelectromech. Syst. **18**, 784 (2009).
[29]A. Massaro, F. Spano, P. Cazzato, R. Cingolani, and A. Athanassiou, Prog. Electromagn. Res. J. **16**, 145 (2011).
[30]E. Finot, A. Passian, and T. Thundat, Sensors **8**, 3497 (2008).
[31]W. Fang and J. A. Wickert, J. Micromech. Microeng. **5**, 276 (1995).
[32]B. Viswanath, C. Ko, and S. Ramanathan, Scr. Mater. **64**, 490 (2011).
[33]J. H. Kim, H. J. Lee, S. W. Han, J. M. Kim, and C. W. Baek, Key Eng. Mater. **321–323**, 121 (2006).
[34]V. Balakrishnana, C. Ko, and S. Ramanathan, J. Mater. Res. **26**, 1384 (2011).